S. Lin, P. Sun, X. Huang (2019) *Can peat soil support a flaming wildfire*? **International Journal of Wildland Fire**, https://doi.org/10.1071/WF19018

Can Peat Soil Support a Flaming Wildfire?

Shaorun Lin[A], Peiyi Sun[A] and Xinyan Huang[A,B,C]

[A]*Research Centre for Fire Engineering, The Hong Kong Polytechnic University, Kowloon, Hong Kong*

[B]*The Hong Kong Polytechnic University Shenzhen Research Institute, Shenzhen, Guangdong, China*

[C]*Corresponding author. Email: xy.huang@polyu.edu.hk*

Corresponding author: Xinyan Huang

Address: ZS832, 181 Chatham Road South, Kowloon, Hong Kong

Email: xy.huang@polyu.edu.hk

Tel.: +852 3400 8286

Fax: +852 2765-7198

Running Head: **Flaming Peat Fire**

Keywords: Peatland; Smoldering; Piloted ignition; Ignition energy; Moisture; Critical heat flux.

Abstract

Smoldering wildfire in peatlands is one of the largest and longest fire phenomena on Earth, but whether peat can support a flaming fire like other surface fuels is still unclear. Our experiments demonstrate the successful piloted flaming ignition of peat soil with moisture up to 100 wt.% under external radiation, indicating that flame may rapidly spread on peatland before transitioning to the conventional smoldering peat fire. Compared to smoldering ignition, flaming ignition of peat is more difficult, requiring a higher minimum heat flux and triple ignition energy. The propensity for flaming increases with a drier peat and a larger external heating. We also found that the flaming ignition temperature increases from 290°C to 690°C, as the peat moisture increases to 100 wt.%. The flame of peat soil is much weaker than that of pine needles and wood, and it eventually transitions to smoldering. The heat of flaming is estimated to be 13 $MJ{\cdot}kg^{-1}$, close to the heat of smoldering. The measured CO/CO_2 ratio of flaming peat fires is less than 0.02, much smaller than 0.2 of smoldering peat fires. This research helps understand the development of peat fire and the interaction between flaming and smoldering wildland fires.

Brief summary

Fire in organic peat soils is often in the form of flameless and slow-spread smoldering, different from conventional flaming wildfires. This work explores if a flame can be piloted above the peat soil under external heating, and then fast spread over peatland surface to rapidly increase the scale of peat fire.

1. Introduction

Wildfire has become a severe global problem which poses severe threats to the safety of human lives and properties as well as the economy and environment (Pel *et al.* 2012). Catastrophic wildfires in recent years reveal a dramatic increase in size, frequency and duration because of climatological and human factors (Liu *et al.* 2010; McClure and Jaffe 2018; Toledo *et al.* 2018), particularly in United States, Australia, Indonesia and many European countries (Gibson *et al.* 2018; Koksal *et al.* 2018). In particular, smoldering wildfires in peatlands are the largest and longest fire phenomena on Earth (Rein 2013). Although peatlands only cover 3% of the Earth land surface, they store around 25% of the planet's terrestrial organic carbon, i.e., approximately the same amount of carbon in the atmosphere (Gorham 1994; Turetsky *et al.* 2015). These peat fires result in the widespread destruction of ecosystems and regional haze event, e.g. recent mega-fires in Southeast Asia, North America and North Europe (Page *et al.* 2002; Rein 2013; Huang and Rein 2017). More importantly, peat fires contribute greatly to the global climate change, as annually they release the ancient carbon that is approximately equivalent to 15% of human-made emissions (Page *et al.* 2002; Ballhorn *et al.* 2009; Turetsky *et al.* 2015).

Peat soil is an accumulation of incompletely decomposed vegetation residues, and it is carbon-rich and formed in anaerobic conditions (Page *et al.* 2002). Peat is also a porous and charring natural fuel that is prone to smoldering combustion like plastic foams and coals (Rein 2013). Once ignited, smoldering peat fires can burn for weeks, months and even years despite extensive rains, weather changes, or firefighting attempts. Most research in the literature have focused on the smoldering characteristics of a peat fire, such as the chemical kinetics (Huang and Rein 2014), smoldering ignition (Frandsen 1987; Hadden *et al.* 2013; Huang *et al.* 2015; Restuccia *et al.* 2017), fire spread (Huang *et al.* 2016; Kreye *et al.* 2016; Prat-Guitart *et al.* 2017; Huang and Rein 2019), extinction (Huang and Rein 2015; Ramadhan *et al.* 2017), and emission gases (Hadden *et al.* 2013; Hu *et al.* 2019). Because most natural fuels can support both smoldering and flaming fires, such as pine needle beds (Wang *et al.* 2016), twigs, bark (Simeoni 2016) and firebrands (Fernandez-Pello 2017), it is logical to expect that peat soil can also support a flaming fire. Pyrolysis that occurs under external heating is the common prerequisite for both flaming and smoldering fires, as illustrated in Fig. 1. When the char oxidation dominates the oxygen consumption (Path I), smoldering fire occurs, while flaming fire is sustained by the oxidation of pyrolysis gases (Path II).

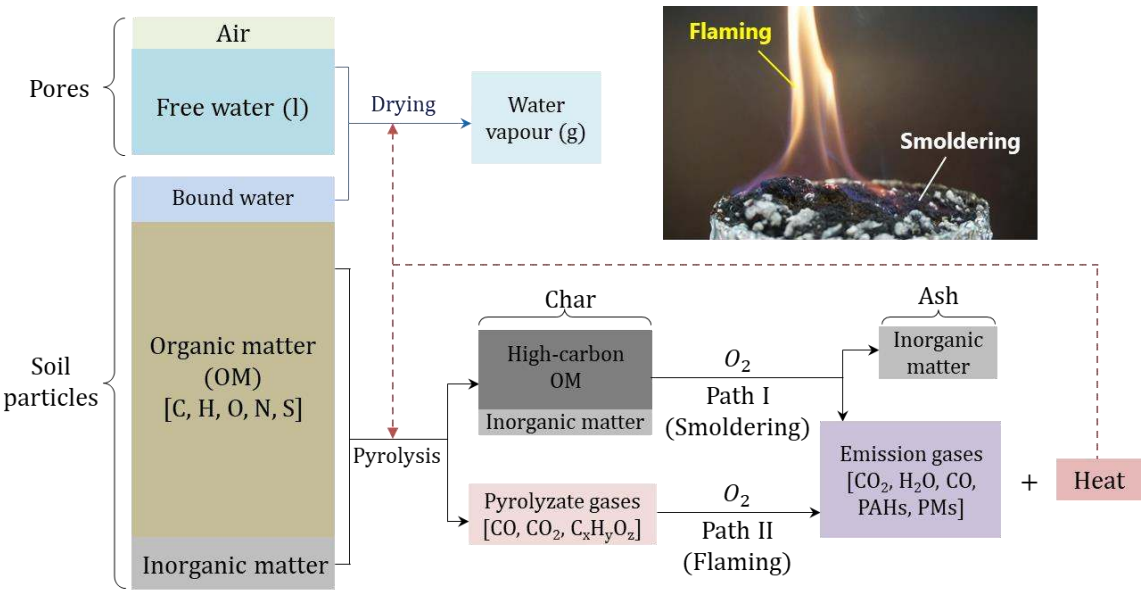

Figure 1. Possible reaction paths for flaming and smoldering combustion of peat soils in wildfires.

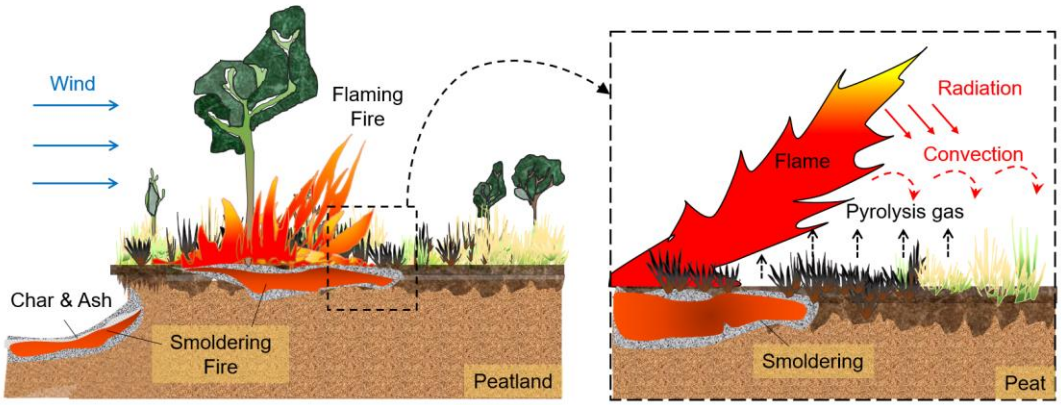

Figure 2. Schematics of flaming and smoldering fires in peatland and the possible piloted flaming ignition of peat soils.

Fundamentally, the flaming fire spread is a continuous ignition process that is heated and piloted by the flame (Williams 1977). If a flame can be piloted on the peat soil, it means that the flame can spread on the peatland surface in a speed much faster than the conventional smoldering spread, resulting in a fast expansion of peat fire. As illustrated in Fig. 2, in real wildfire scenarios, the flame of burning grasses or trees can act as the heating and pilot sources, causing the piloted flaming ignition of peat soils. In turn, the pyrolysis gases generated from the peat, can also support the flaming wildfire via Path (II) in Fig. 1. For different wildland fuels, propensities for flaming and smoldering fires are different. For example, grass, leaves, and twigs are prone to flaming fire, while ember, duff, and peat may be more likely to smolder. Nevertheless, theoretically all charring fuels can support both forms of fires which can also transition to each other under specific conditions, but relevant studies are quite limited. Traditionally, smoldering spreads in a creeping fashion, typically around O(1) cm·h^{-1}, which is at least two orders of magnitude slower than the spread rate of flaming fires (Rein 2013). However, if flame can spread over the surface of peat soil, the size of peat fire can expand much faster than the expected creeping smoldering spread inside the peat layer. So far, no research has studied the critical conditions of flaming ignition of peat and the propensity for a flaming fire spreading on peatlands, so there is a big knowledge gap.

For many fuels, smoldering could be easier to initiate than flaming (Rein 2014). For a low-density (20 kg·m^{-3}) polyurethane (PU) foam, the minimum radiant heat flux for smoldering ignition is 7 kW·m^{-2}, while for flaming ignition, it is 13 kW·m^{-2} with a pilot igniter and 30 kW·m^{-2} without an igniter (Hadden *et al.* 2012; Rein 2014). However, smoldering ignition could be more difficult for trees and twigs. For a redwood (~350 kg·m^{-3}), if the heat flux is larger than 40 kW·m^{-2}, the required heating time and surface temperature for piloted flaming ignition are lower than for smoldering ignition (or glowing) (Boonmee and Quintiere 2002). Whether it is easier to pilot a flame and support flame spread over a common peat soil (~200 kg·m^{-3} dry density) is still unclear. Moreover, peat, as a typical wildland fuel, can hold a wide range of moisture contents[1] (MCs), from 10~50% under drought conditions to well above 300% under flooded conditions (Watts 2012; Huang and Rein 2015). MC is also expected to alter the propensity of wildland fuels for flaming or smoldering (Valdivieso and Rivera 2013; Wang *et al.* 2016).

Many past works have investigated the flaming ignition of wildland fuels like foliage and pine needles with MCs of 3~300% under wildfire intensity up to 10^3 kW·m^{-2} or above 10^5 W·m^{-1} (Finney *et al.* 2013; Jervis and Rein 2015). Several studies found for many wildland fuels, the piloted flaming ignition time under external heating increased almost linearly with the fuel MC, and there was a maximum MC above which flaming ignition could not occur (Dimitrakopoulos and Papaioannou 2001; McAllister *et al.* 2012; Wang *et al.* 2016). Besides MC, whether the wildland fuel is fresh, aged, or dead has a significant impact on the flammability (Jervis and Rein 2015). Many ignition theories have been proposed based on the critical ignition temperature, ignition energy, and critical mass flux (Drysdale 2011). These theoretical work reasonably well for common dry polymer

[1] Moisture content (MC) is defined in dry basis as the mass of water divided by the mass of a dry soil sample, expressed as a percentage (wt.% or %).

materials but become less reliable for complex wildland fuels (Lyon and Quintiere 2007; McAllister 2013; Wongchai and Tachajapong 2015), thus, requiring a better ignition criterion.

In this work, the flaming ignition with a pilot source and smoldering ignition of peat is investigated under varying MCs (10 ~ 100%) and exposed to radiant heat fluxes (5 ~ 90 kW·m^{-2}). The ignition delay time, mass flux, CO/CO$_2$ ratio and minimum heat flux are quantified for both flaming and smoldering ignition of peat.

2. Experiment

2.1. Apparatus and peat sample

All ignition experiments were conducted using the cone calorimeter (FTT iCone Plus) (Babrauskas 2016). The cone-shape heater can provide a constant heat flux to the sample area of 10 cm ×10 cm. The schematic diagram of the experimental apparatus is illustrated in Fig. 3 (a), and it mainly consists of a cone-shape heater, a cylindrical sample container, a precision scale (± 1 mg), and a spark igniter.

The carbon-rich peat soil tested in the experiment is the moss peat from the Netherlands (Fig. 3b), and it has an organic matter content of about 96%. The element analysis for the peat organic matter shows 44.2/6.1/49.1/0.5/0.1% mass fraction for C/H/O/N/S, respectively. The peat was first oven-dried at 90°C for 48 h (Huang and Rein 2017), and the oven-dried bulk density of peat was measured as 145 kg·m^{-3} (MC → 0%). In general, the drying process weakens the hydrophilicity of peat, but it does not affect the high-temperature pyrolysis and smoldering processes (Perdana *et al.* 2018). The peat bed has an open-pore structure and a porosity of about 0.90, considering a solid density of 1500 kg·m^{-3} (Jacobsen *et al.* 2003). When the oven-dried peat was in contact with air, it quickly absorbed ambient moisture and reached a new equilibrium with about 10% MC, defined as the air-dried peat (Huang *et al.* 2016). In order to obtain other MCs, the oven-dried peat was mixed with water by following the same process in Huang *et al.* (2016). For example, 2 kg of 100% MC peat can be produced by mixing 1 kg of dry peat with 1 kg of water. Afterwards, samples were shaken to enhance the mixing process and left into the sealed boxes for homogenization for at least 48 h. The other two targeted MCs for peat were 50% (drought) and 100% (wet).

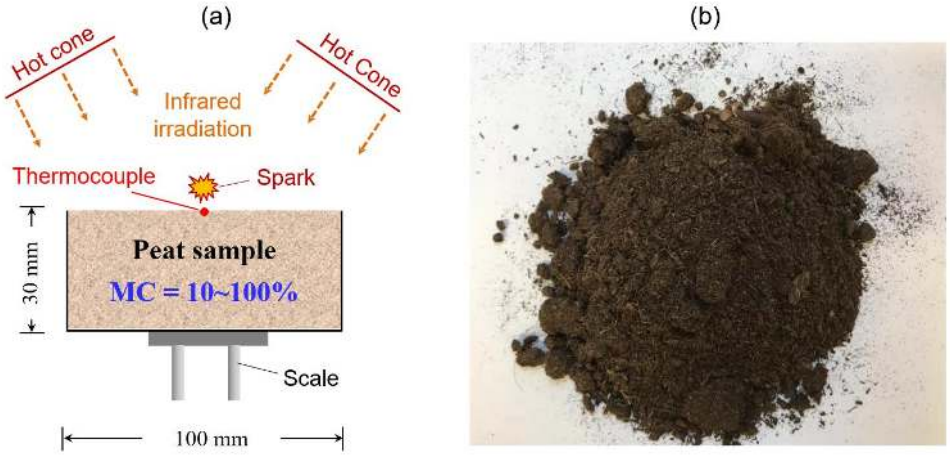

Figure 3. (a) Schematic diagram of the cone calorimeter and sample, and (b) photo of moss peat sample.

The cylindrical container (with a diameter of 100 mm and a height of 30 mm) was made of metal mesh, so aluminum foil was placed between the peat and container to prevent oxygen leakage from the side and bottom. During the water absorbing process, the volume of peat sample tended to expand naturally (Huang and Rein 2017). To avoid this issue, after filling in, moist samples were compressed manually to ensure the dry bulk density of peat was fixed to 145 kg·m^{-3}, regardless of the MC. The bulk densities of peat samples with different MCs are listed in Table 1. During the test, the ambient temperature was 22 ± 2 °C, and the humidity of 50 ± 10%, and the ambient pressure was 1 atm.

2.2. Ignition methods

For the piloted ignition, the cone temperature was varied for producing various radiant heat flux ($\dot{q}''_r$) from 5 kW·m^{-2} to 90 kW·m^{-2}. As illustrated in Fig. 3 (a), the spark was inserted and placed at 5 mm above the top surface of the peat sample prior to heating. In real wildland fires, flaming embers or surface fires can act as the piloted source for the peat soils, as shown in Fig. 2. In experiment, the radiant heating started once the shield of cone heater was removed. The surface temperature of peat was carefully monitored using two K-type thermocouple (0.5 mm bead diameter) that was in contact with the peat top surface. The moment of flaming ignition ($t_{ig,f}$) and the following burning process were captured by a video camera. Once the flaming ignition occurred, the spark was removed while the heating was continued until the sample mass no longer changed (or burnout). A failed flaming ignition was considered if the flame did not occur after heating for 10 min. Then, the radiant heat flux was adjusted to find the minimum heat flux for flaming ($\dot{q}''_{min,f}$). Throughout the experiment, flaming autoignition, i.e., the smoldering peat fire self-transitioning to flaming fire without a spark, was not observed.

For the smoldering ignition, the piloting spark was removed under the same radiant heat flux. The peat sample was placed under the cone heater for a prescribed heating duration, and then, moved to the nearby fume hood. Unlike the flaming ignition, it was not possible to instantaneously and visually determine the success of smoldering ignition. Thus, the sample was left for another half an hour to observe if a stable smoldering was successfully initiated, e.g. strong smoke released from the sample, visual hot spots or burnout. If successful, the heating time was reduced until the minimum time for smoldering ignition ($t_{ig,sm}$) was found. Typically, the release of smoke was also observed during the heating for a smoldering ignition, but the amount of smoke was not enough to pilot a flame. Like the flaming ignition, the radiant heat flux was adjusted to find the minimum heat flux for the smoldering ignition ($\dot{q}''_{min,sm}$). For both ignition forms, 3~5 repeating experiments were conducted to obtain the average ignition time.

Table 1. Average values and standard deviations of bulk density, minimum ignition heat flux, ignition temperature, and ignition energy of peat soils of different MCs, where the dry bulk density of peat is fixed to 145 kg·m^{-3}, where symbols are explained in Appendix 1.

Fire	Parameters	MC = 10% (air-dried)	MC = 50% (drought)	MC = 100% (wet)
Smoldering	ρ [kg·m^{-3}]	160	218	290
	$T_{ig,\,sm}$ (°C)	270 ± 5	275 ± 10	280 ± 5
	$\dot{q}''_{min,sm}$ [kW·m^{-2}]	6.5 ± 0.5	6.5 ± 0.5	6.5 ± 0.5
	$\dot{q}''_{min,sm,cal}$ [#] [kW·m^{-2}]	6.3 ± 0.2	6.6 ± 0.5	6.8 ± 0.3
	$E_{ig,sm}$ [MJ·m^{-2}]	0.10 ± 0.02	0.39 ± 0.03	0.65 ± 0.08
Flaming	$T_{ig,\,f}$ (°C)	285 ± 5	590 ± 10	690 ± 10
	$\dot{q}''_{min,f}$ [kW·m^{-2}]	7.5 ± 0.5	43 ± 2	53 ± 2
	$\dot{q}''_{min,f,cal}$ [#] [kW·m^{-2}]	7.1 ± 0.5	35 ± 1	52 ± 1
	$E_{ig,f}$ [MJ·m^{-2}]	0.30 ± 0.05	1.1 ± 0.12	2.0 ± 0.21
	$\dot{m}''_{min,f}$ [g·m^{-2}·s^{-1}]	4.3 ± 0.1	7.9 ± 0.3	10.4 ± 0.4

*Oven-dried peat cannot be tested as it quickly absorbs the ambient water to reach a new equilibrium.
[#]Calculated using the measured T_{ig} and the thermal equilibrium in Eq. (1).

3. Results and discussions

3.1. Peat's propensity for flaming and smoldering

Figure 4 shows an example of the piloted flaming ignition process of peat soil under a high radiant heat flux of 70 kW·m^{-2} with different MCs. The original videos can be found in the Supplemental Materials (Videos 1-3). The average ignition time of several repeating tests for smoldering ignition and piloted flaming ignition are indicated in Fig. 4 as well. During the heating process, smoke was always observed before any form of ignition, and this visible smoke should be a mixture of water vapor and pyrolysis gases. Continuing the heating,

smoldering ignition was first achieved, and then, a flame could be piloted, if the heating flux was larger than the minimum value for flaming ignition (Table 1). Therefore, we can conclude that peat soils can support a flaming wildfire under external radiation, even when the fuel MC as high as 100%, thus, it is similar to other wildland fuels like leaves, twigs, and bark. In other words, the flame can spread over peat soils because the spread of flame is a process of continuous piloted ignition. Note that as the peat MC is increased, the intensity of flame becomes weaker (see Fig. 4), discussed more in Section 3.4.

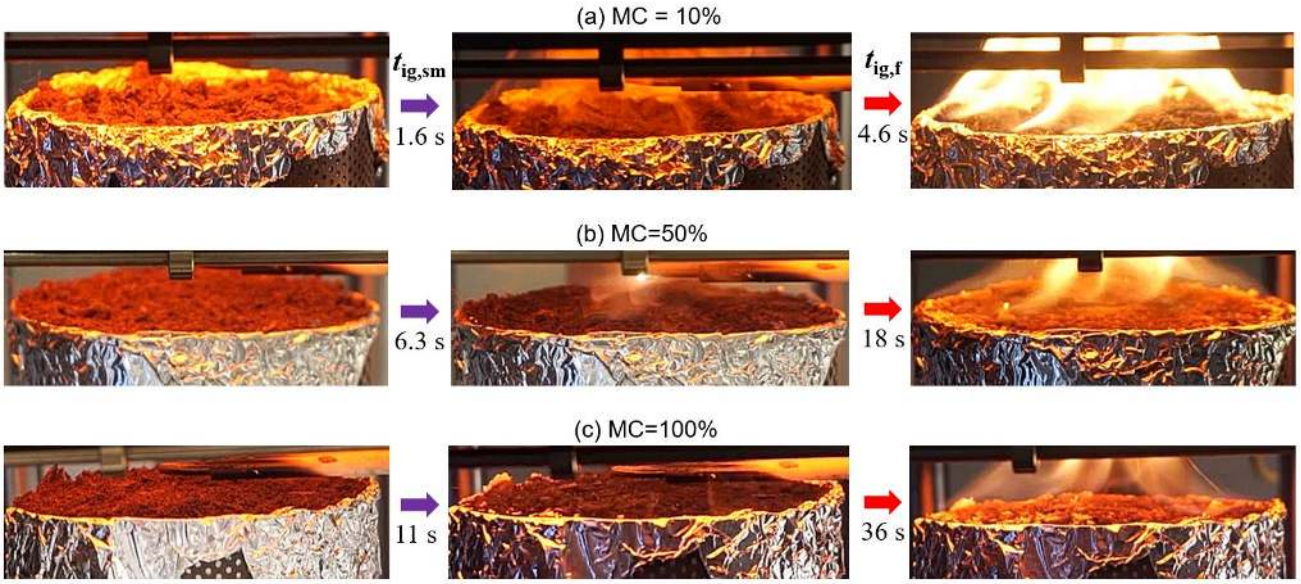

Figure 4. Pilot flaming ignition process of peat under the radiant heat flux of 70 kW·m^{-2}, (a) MC = 10%, (b) MC = 50%, and (c) MC = 100%, where the average ignition time for smoldering and flaming are provided. See Videos 1-3 in the Supplemental Materials.

By plotting the ignition time of flaming ($t_{ig,f}$) and smoldering ($t_{ig,sm}$) versus radiant heat flux in Fig. 5, the propensity of air-dried and wet peat for flaming and smoldering ignition can be quantified. Like all other ignition phenomena, the required heat time decreased with increasing radiant heat flux (McAllister 2013). More importantly, as the heating duration and heat flux decrease, there are three ignition regions,

(I) piloted flaming ignition,

(II) smoldering ignition, and

(III) no ignition.

Clearly, the longer heating duration and larger heat flux are required to initiate the flaming combustion of peat soil. Therefore, the propensity of peat soil for smoldering is greater than that of flaming. This behavior is the same as the low-density PU foam (Hadden *et al.* 2012; Rein 2014), while unlike the high-density redwood, probably because peat has a relatively small bulk density (160 kg/m^3 for air-dried peat) and a similar open-pore structure like PU foam.

For the air-dried peat (MC = 10%) in Fig. 5(a), under the same radiant heat flux, only a slightly longer heating duration is required for flaming than for smoldering. For example, under $\dot{q}''_r = 30$ kW·m^{-2}, a heating time of 5.5 ± 0.5 s is required for smoldering ignition, and 12.5 ± 0.6 s is required for piloted flaming ignition. Nevertheless, both ignition forms are relatively easy to achieve (i.e., very small Region II), and the minimum heating flux for flaming ignition is $\dot{q}''_{min,f}$ = 7.5 ± 0.5 kW·m^{-2}, and for smoldering ignition, it is only slightly smaller as $\dot{q}''_{min,sm}$ = 6.5 ± 0.5 kW·m^{-2}.

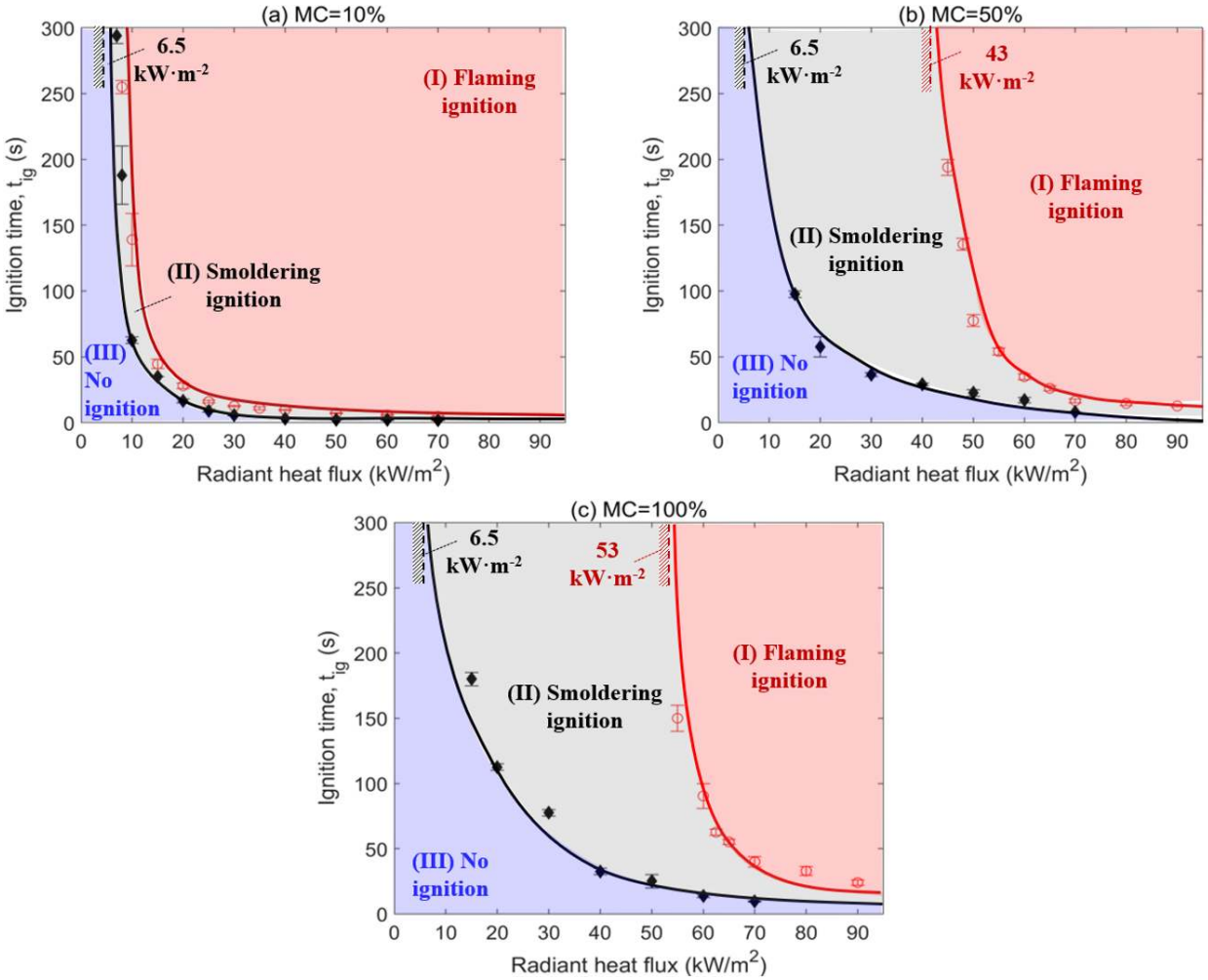

Figure 5. The ignition delay time for piloted flaming ignition and smoldering ignition for (a) air-dried peat sample (MC = 10%), (b) drought peat sample (MC=50%), and (c) wet peat sample (MC = 100%), where three ignition regions (I-III) are identified. The symbols show the experimental data (with standard deviations), and lines are manual fitting curves.

For the wet peat (MC =100%) in Fig. 5(c), the minimum heat flux for smoldering ignition ($\dot{q}''_{min,sm}$) approaches to 6.5 kW·m^{-2} that is the same as the air-dried peat in Fig. 5(a), because the wet peat will be eventually dried by the long-term heating. On the other hand, the minimum heat flux for flaming ignition ($\dot{q}''_{min,sm}$) increases significantly to 55 kW·m^{-2}. For Region II with the heat flux between 6.5 and 53 kW·m^{-2}, only smoldering ignition can take place, and even if the spark is kept during the continuous heating, flaming will not occur, and the peat is burnt out by smoldering. Therefore, as the peat MC is increased, the propensity for flaming is decreased significantly. Moisture has three effects on the peat: (1) changing the thermal properties of the material (density, thermal conductivity, and specific heat increases, as shown in Table 1), (2) enhancing the heat transfer via molecular diffusion, and (3) acting as a strong heat sink during evaporation (McAllister *et al.* 2012). Therefore, for the wet peat, a higher heating intensity is needed to trigger the flaming ignition, and the propensity for flaming is significantly decreased.

3.2. Flaming ignition limit of peat

For the piloted flaming ignition, Fig. 6(a) further compares the ignition delay time and the minimum heat fluxes ($\dot{q}''_{min,f}$) for different peat MCs. The measured ignition temperatures are listed in Table 1 and shown in Fig.6(b). As the peat MC is increased from 10% (air-dried) to 50% (drought) and 100% (wet), the required minimum heat flux increases from 7.5 kW·m^{-2} to 43 kW·m^{-2} and 53 kW·m^{-2}, respectively; and the ignition temperature increases from 285 ℃ to 590 ℃ and 690 ℃, respectively. As expected, the measured flaming ignition temperature for dry peat (285 ℃) is close to the peat pyrolysis point (see TGA curves in the Appendix 2), and it is higher than the 270 ℃ found for smoldering, similar to many other fuels with a low density and a

high porosity (Rein 2014). However, a significant increase of ignition temperature due to moisture is unexpected.

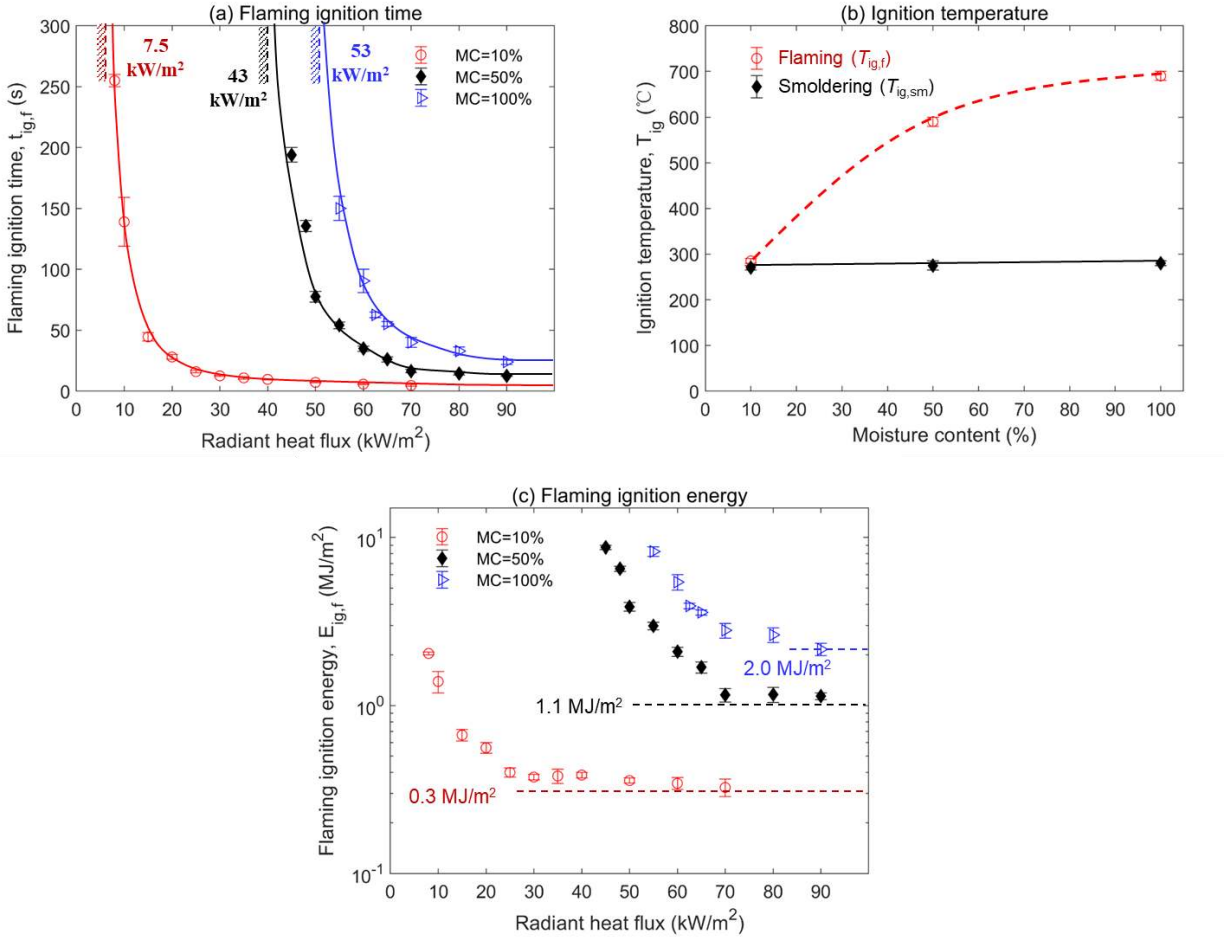

Figure 6. Piloted flaming ignition of peat soil sample under different radiant heat flux and MCs, (a) the flaming ignition time, (b) the surface ignition temperature for flaming and smoldering, and (c) the flaming ignition energy by using Eq. (3), where the horizontal lines indicate the minimum ignition energy. The symbols show the experimental data (with standard deviations), and the lines are the manual fitting curves.

In order to verify the measurement of ignition temperature and minimum heat flux, a simple calculation based on thermal equilibrium is proposed. Based on the definition (Quintiere 2006), the minimum heat flux should balance the environmental heat loss right below the ignition temperature (T_{ig}) as

$$\dot{q}''_{min} = \dot{q}''_{loss} = \varepsilon\sigma\left(T_{ig}^4 - T_a^4\right) + h\left(T_{ig} - T_a\right) \quad (1)$$

where $\varepsilon = 0.9$ is the emissivity of peat; $\sigma = 5.67 \times 10^{-8}$ J·m^{-2}·s^{-1}·K^{-4} is the Stefan–Boltzmann constant; T_a is the ambient temperature. The free-convection heat transfer coefficient (h) for a horizontal hot plate can be estimated by an empirical equation (Holman 1990) as

$$h = 1.52\left(T_{ig} - T_a\right)^{1/3} \quad (2)$$

Then, the minimum heat flux can be calculated ($\dot{q}''_{min,f,cal}$) based on the measured flaming ignition temperatures ($T_{ig,f}$), as listed in Table 1, which shows a good agreement with the measured minimum heat flux. Thus, we confirm the reliability of the measured ignition temperature and minimum heat flux.

In the literature, although the piloted ignition temperature has been found to change with environment (e.g. heat flux and air flow) and fuel conditions (e.g. MC and density) (Zabetakis 1965; Janssens 1991; Babrauskas 2001; Boonmee and Quintiere 2002; Lyon and Quintiere 2007; Rich *et al.* 2007; McAllister 2013; Wongchai and Tachajapong 2015), the variation is relatively small (<50°C), and most of the fuels have a low MC (<30%). Therefore, it is reasonable to assume that the piloted flaming ignition temperature for a given fuel is nearly a

constant and slightly above the fuel pyrolysis point (Quintiere 2006). Comparatively, the change of ignition temperature found in this work is as large as 300°C (see Fig. 6b), and such change should be attributed to the much higher MC and peat's strong tendency to smoldering (explained more in Section 3.3). Therefore, the assumption of near-constant flaming ignition temperature completely fails for the wet wildland fuels like peat, that can hold a wide range of MCs, even reach above 300%.

At the same time, the ignition energy provided by the cone heater can be simply calculated as

$$E''_{ig} = \dot{q}''_r t_{ig} \tag{3a}$$

The ignition energy for piloting a flame on peat is plotted in Fig. 6(c). When the radiant heat flux is much larger than the heat loss ($\dot{q}''_r \gg \dot{q}''_{loss}$), the minimum ignition energy per unit area (E''_{min}) can be estimated as

$$E''_{min} = \dot{q}''_{r,max} t_{ig} \tag{3b}$$

The minimum flaming ignition energy ($E''_{min,f}$) for different peat MCs is shown as the trendline in Fig. 6(c) and listed in Table 1. In particular, the minimum energy increases almost 7 times from 0.3 MJ/m^2 to 2.0 MJ/m^2, as the peat MC is increased from 10% to 100%, because additional energy is required to heat and evaporate the soil water (McAllister 2013). Moreover, it is found that regardless of the peat MC, the minimum ignition energy for flaming is about 3 times of that for smoldering, as shown in Table 1. As demonstrated in our previous work and numerical model (Huang and Rein 2015; Huang *et al.* 2015), the peat moisture content, inorganic content, and density are most important parameters for peat ignition.

3.3. Critical mass flux for flaming ignition

For the piloted flaming ignition, the critical mass flux (or mass loss rate per unit area, $\dot{m}''_{ig,f}$) is considered as one of the most fundamental criteria (Rich *et al.* 2007). It is because the value of mass flux is more related to the profile of fuel concentration and the flammability region above the fuel surface. Nevertheless, the importance of critical mass flux also indicates its sensitivity to the location of the piloted source (Drysdale 2011). In contrast, the mass flux may not be appropriate to characterize the moment of smoldering ignition, because smoldering is dominated by heterogenous oxidations in the solid phase, rather than the mixing process and flammability limit in the gas phase.

The mass flux was computed as the time differentiation of the original sample mass measurements. Figure 7(a-c) shows some examples of the measured mass flux time evolution during the entire ignition and burning process of peat, where the symbol indicates the moment of piloted flaming ignition and the critical mass flux. The scrutiny reveals very different locations of the ignition moment in the mass flux curve of different MCs. It is particularly clear in Fig. 7(c) that the flaming ignition occurs in the ascending period for the air-dried peat (MC = 10%), near the peak mass flux for the drought peat (MC = 50%), and in the descending period for the wet peat (MC = 100%). For any wet fuel, the measured overall mass flux includes both the water vapor due to drying ($\dot{m}''_w$) and the pyrolysis gas due to the peat degradation ($\dot{m}''_{py}$) as

$$\dot{m}'' = \dot{m}''_w + \dot{m}''_{py} \tag{4}$$

Because of the low evaporation point, the mass flux of water vapor most likely contributes to the initial stage as well as the peak in the total mass flux.

When the heat flux is relatively small, for example in Fig. 7(a-b), the water both near the surface and in-depth will first evaporate. When the top surface just reaches the pyrolysis point, there is still a large flux of water vapor from the sample in-depth which alters the flammability limit at the location of the pilot spark. Thus, despite a large overall mass flux ($\dot{m}''$), no flaming ignition occurs because of a small mass flux of the pyrolysis gas ($\dot{m}''_{py}$). As the heating continues, both $\dot{m}''_w$ and $\dot{m}''_{py}$ start to decrease, because the reaction front moves in-depth, and the char layer forms on the sample surface to block the radiant heating. At the same time, the continuous heating initiates a robust smoldering fire that dominates the following burning process. However, gas products from smoldering emissions, i.e., mostly H_2O, CO_2, and CO (Hadden *et al.* 2013; Hu *et al.* 2019), are not large and flammable enough to pilot a flame. Therefore, throughout the heating process, the mixture of

air, the water vapor, and pyrolysis gases near the spark never exceeds the lower flammability limit unless $\dot{q}''_{min,f}$ is reached. This is the fundamental reason why the minimum heat flux for flaming ignition (Fig. 6(a)) as well as the area of Region II (Fig. 5) increases with the fuel MC. More detailed numerical simulations with both gas-phase and solid-phase processes are needed to quantify the time evolution of $\dot{m}''_w$ and $\dot{m}''_{py}$ and the minimum heat flux.

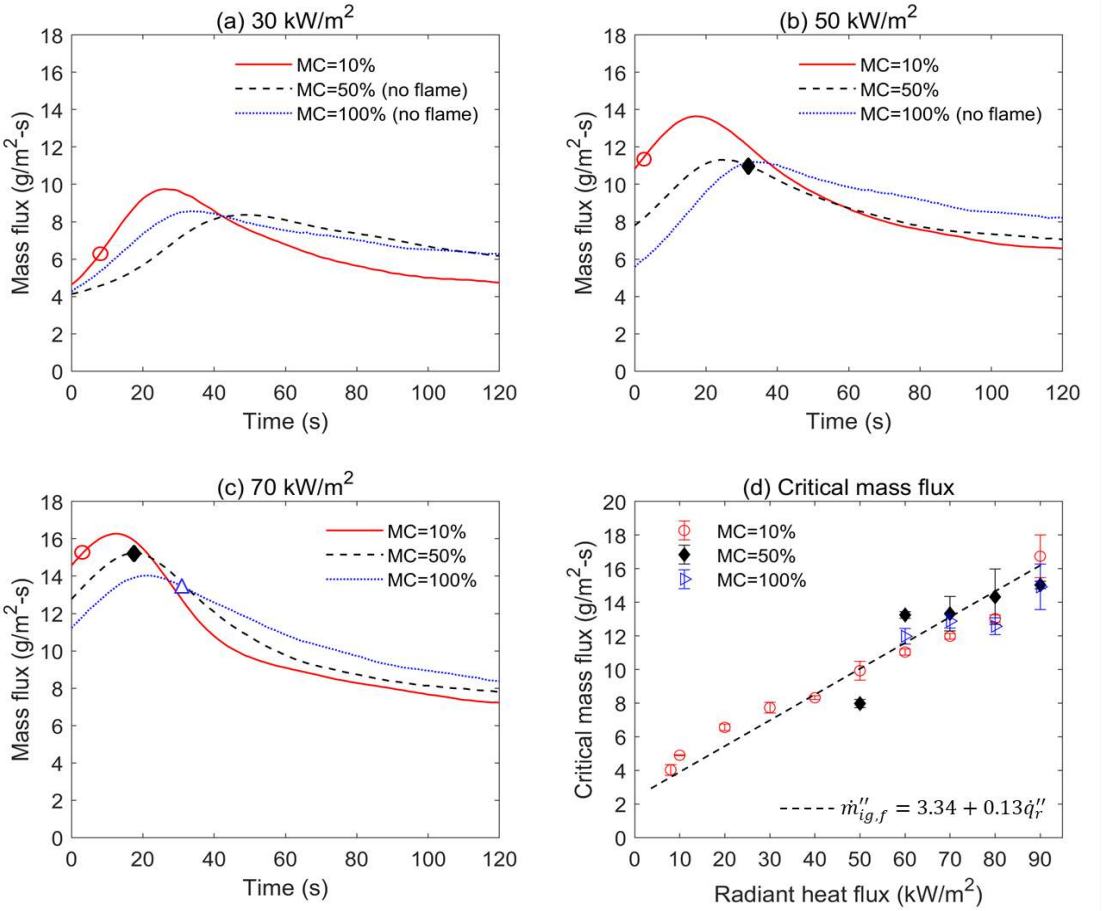

Figure 7. Time evolution of mass flux under the radiant heat flux of (a) 30 kW/m^2, (b) 50 kW/m^2, and (c) 70 kW/m^2, where the symbol indicates the moment of the piloted flaming ignition of peat, and (d) critical mass flux for piloted flaming ignition ($\dot{m}''_{ig,f}$) under all radiant heat fluxes and peat MCs, where the symbols show the experimental data (with standard deviations), and the dashed line is the result of OLS regression.

Figure 7(d) summarizes the average critical mass flux of repeating tests under various MC and radiant heat flux, where the symbols show the experimental data and the error bars show the standard deviations. Interestingly, the critical mass flux is found to increase almost linearly with the radiant heat flux up to 90 kW/m^2. In particular, the $\dot{m}''_{ig,f} = 4.9$ g·m^{-2}·s^{-1} at 10 kW·m^{-2} while it increases more than 3 times to 16.8 g·m^{-2}·s^{-1} at 90 kW·m^{-2}. Then, an empirical correlation based on OLS regression can be fitted for all data points of different MCs as

$$\dot{m}''_{ig,f} = 3.4 + 0.13\dot{q}''_r \quad (5)$$

where $\dot{m}''_{ig,f}$ has a unit of g·m^{-2}·s^{-1}, and $\dot{q}''_r$ has a unit of kW·m^{-2}. The R^2 coefficient is found to be 0.97, indicating excellent linearity. Such an increase with the radiant heat flux has also been observed for PMMA (polymethyl methacrylate), the most widely used plastic material in fire research, up to $\dot{q}''_r$ = 24 kW·m^{-2} (Rich *et al.* 2007), and wet wood up to $\dot{q}''_r$ = 50 kW·m^{-2} (McAllister 2013). So far, the reason for such a trend has not been well explained yet.

As the peat MC increases from 10% to 100% in Fig. 7(d), the minimum mass flux for flaming ignition ($\dot{m}''_{min,f}$) is also increased from 4.3 g·m^{-2}·s^{-1} to 10.4 g·m^{-2}·s^{-1}, as also listed in Table 1. More importantly, under

the same radiant heat flux, the critical mass flux is found to be insensitive to the peat MC, which has not been observed before. All these abnormal phenomena suggested that care should be taken in using a fixed critical mass flux to describe the flaming ignition of wet wildland fuels (Janssens 1991; McAllister 2013).

3.4. Characteristics of peat flame

Once a flame is ignited and attached to the peat, stable burning is achieved. Based on the principle of oxygen calorimetry, the heat release rate per unit area ($\dot{Q}''$) or HRR can be calculated to quantify the intensity of peat flame, as shown in Eq. (6) (Drysdale 2011):

$$\dot{Q}'' = \left(0.21 - X_{O_2}\right) V_a \rho_{O_2} \Delta H_{ox} / A \tag{6}$$

where V_a is the volumetric flow rate of air ($m^3 \cdot s^{-1}$), ρ_{O_2} is the density of oxygen ($kg \cdot m^{-3}$) at the normal temperature and pressure; X_{O_2} is the mole fraction of oxygen in the 'scrubbed' gases (removing water vapor and acid gases); $\Delta H_{ox} \approx 13.1$ MJ/kg is the heat of oxygen for hydrocarbon-based fuel (Huggett 1980); and A is the cross-section area of the sample, respectively.

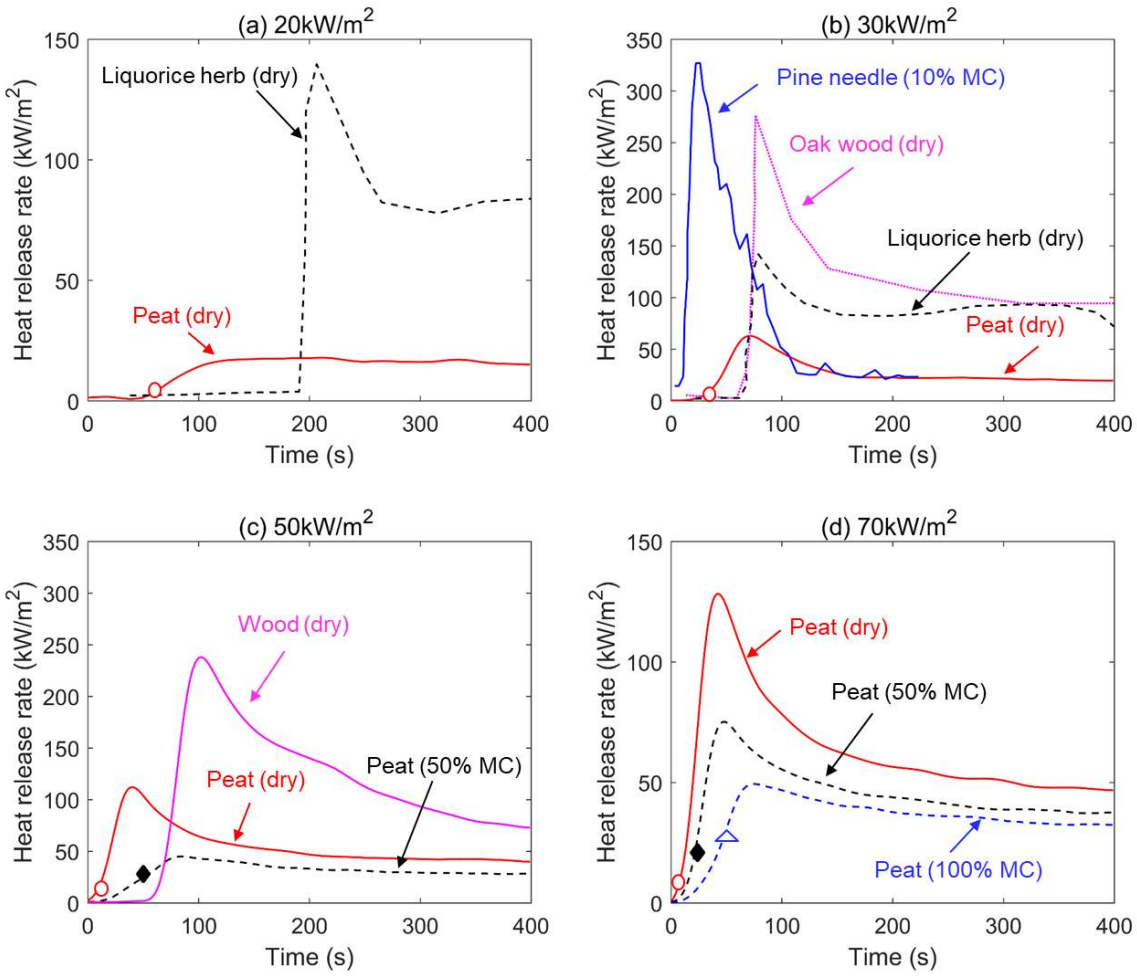

Figure 8. Time evolution of the heat release rate under radiant heat flux of (a) 20 $kW \cdot m^{-2}$, (b) 30 $kW \cdot m^{-2}$, (d) 50 $kW \cdot m^{-2}$, (d) 70 $kW \cdot m^{-2}$, where data of dry wood (Chung and Spearpoint 2008; Zachar *et al.* 2014), liquorice herb (Pei *et al.* 2014), and pine-needle bed (Jerry Alexander *et al.* 2016; Thomas *et al.* 2017) under the same heat flux are presented for comparison.

Figure 8 shows some examples of the flame heat release rate under different radiant heat fluxes and peat MCs. To better compare with the flame intensity of other wildland fuels, the HRR curves of dry wood (Chung and Spearpoint 2008; Zachar *et al.* 2014), liquorice herb (Pei *et al.* 2014) and pine needle beds (Jerry Alexander *et al.* 2016; Thomas *et al.* 2017) are also plotted in Fig. 8(a-c). The comparison shows that once ignited, the

flame intensity of peat is much lower than those of other wildland fuels. For example, in Fig. 8(b) under 30 $kW \cdot m^{-2}$, the peak HRR of dry peat is about 20% of dry pine needle, 24% of oak wood, and 45% of liquorice herb. Moreover, as compared in Fig. 8(d), as the MC is increased from 10% to 100%, the intensity of the flame is reduced by about 60%, consistent with visual observations in Fig. 4 and videos. Therefore, for wet fuel, more than half of the mass loss is attributed to water vapor. As a result, the flame temperature decreases as the mass flux of water vapor increases, so the flame becomes weak and easy to extinguish.

The effective heat of (flaming) combustion (Drysdale 2011) can be estimated from the heat release rate and the mass flux as

$$\Delta H_f = \frac{\dot{Q}''}{\dot{m}''} \tag{7}$$

Calculation shows that ΔH_f =18.4 ± 1.7 $MJ \cdot kg^{-1}$ for the pyrolysis gases of dry peat. Thermogravimetric analysis (TGA) shows that the pyrolysis of peat produces about 70% of pyrolysis gas and 30% black char (see Fig. 1). Thus, the heat of flaming combustion of dry peat is about 18.4 × 0.7 = 13 $MJ \cdot kg^{-1}$.

The heat of smoldering combustion (ΔH_{sm}) can be measured from the differential scanning calorimeter (DSC). For this peat, ΔH_{sm} is measured to be about 12 $MJ \cdot kg^{-1}$ (see Appendix 2 for more details), which is close to 14.2 $MJ \cdot kg^{-1}$ of similar peat previously measured by Frandsen (Frandsen 1991), but higher than 10 $MJ \cdot kg^{-1}$ for wood (Drysdale 2011). Therefore, we can conclude that for this organic-rich peat soil, the heat of flaming and the heat of smoldering are comparable. Also, the total heat of combustion for peat is approximately the combination of flaming and smoldering, i.e., 13 + 12 = 25 $MJ \cdot kg^{-1}$. This value is similar to methanol and ethanol (Thomas 2000), while slightly lower than a typical coal (about 30 $MJ \cdot kg^{-1}$) (Tan *et al.* 2006), considering peat soil is often called as "young" coal.

Note that the HRR from the flame is not only controlled by the heat of flaming combustion, but also by factors influencing the mass loss such as the pyrolysis point, density and porosity of fuel (Quintiere 2006). In fact, the heat of flaming combustion of peat is only slightly lower than that of the pine needle and wood (both about 20 $MJ \cdot kg^{-1}$ (Quintiere 2006), but the HRR of peat is much lower, as compared in Fig. 8. For wood, its high density allows for more gaseous fuels released per unit area (i.e., larger fuel mass flux), while for pine needle beds, the flame can be sustained in the larger pores and heat each piece of pine needle, both of which make the flame heating more effective. Comparatively, for peat, (1) the flame cannot be sustained inside the pore; (2) the bulk density is small; and (3) heat of flaming is lower, so all these three factors make the flame weaker on peat soils.

3.5. Carbon emission from peat fires

Peatlands play an important role in the global carbon balance and recent environmental changes (Page *et al.* 2002; Turetsky *et al.* 2015). For example, the 1997 peatland fires in Indonesia may have released 13–40% of the mean annual global carbon emissions from fossil fuels (Page *et al.* 2002). More importantly, compared to regular flaming wildland fires, the amount of toxic carbon monoxide (CO) released from smoldering peat fires is much higher. Laboratory measurements have shown that if 1 kg of dry peat is burnt in smoldering, 0.17~0.25 kg of CO is released (i.e., a CO emission factor of 0.17~0.25 $kg \cdot kg^{-1}$), and the CO/CO_2 ratio is between 0.15 and 0.43 (Rein *et al.* 2009; Hu *et al.* 2018, 2019). Comparatively, the emission factor of CO for flaming wildland fuel is less than 0.02 $kg \cdot kg^{-1}$ (Grexa and Lübke 2001), and the CO/CO2 ratio is less than 0.03 (Schemel *et al.* 2008; Fateh *et al.* 2016).

Figure 9 plots the typical time evolution of CO/CO_2 ratio for smoldering and flaming peat fire under different MCs and external radiation. The solid symbol indicates the moment of flame ignition, and the hollow symbol indicates the moment of flame extinction and smoldering peat fire. Based on the change in CO/CO_2 ratio, three stages of peat fire can be observed:

1) Before the flaming ignition or during drying and pyrolysis, the carbon emission through CO increases, and the CO/CO_2 ratio is high (0.1~0.35);
2) Once flaming ignited, the CO emission starts to decrease, and the CO/CO_2 ratio decreases to about 0.02 which is similar to other flaming wildland fires (Schemel *et al.* 2008; Fateh *et al.* 2016). In general, the

duration of flame lasts longer under larger external radiation;

3) After flame extinction, there is a continuation of smoldering, and the CO/CO_2 ratio increases to about 0.2 until burnout, similar to past measurements in (Rein *et al.* 2009; Hu *et al.* 2018, 2019).

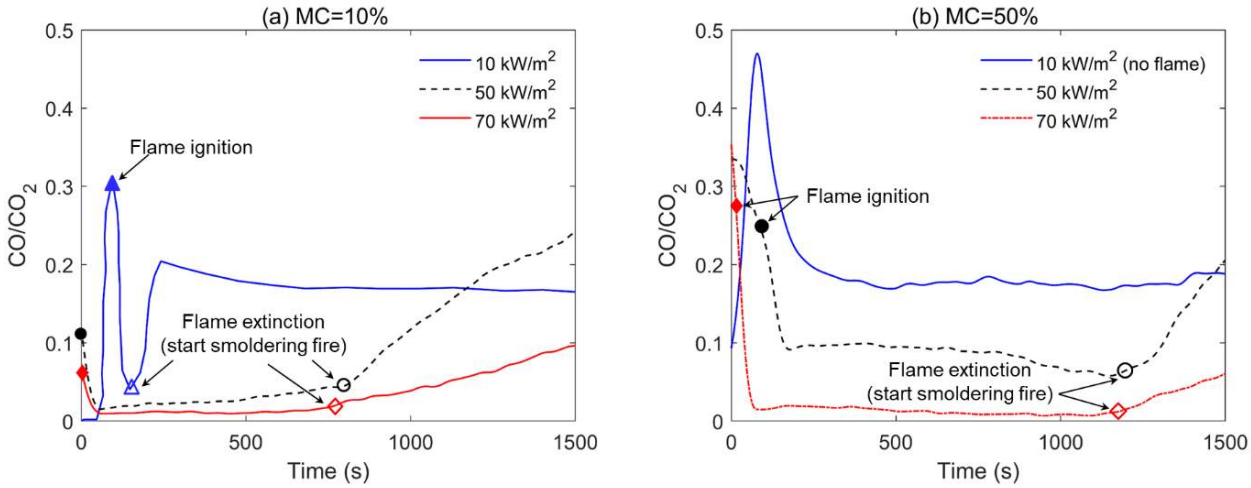

Figure 9. Time evolution of CO/CO_2 ratio under different external heat fluxes with the peat moisture content (MC) of (a) 10% and (b) 50%, where the solid symbol indicates the moment of flame ignition, and the hollow symbol indicates the moment of flame extinction and smoldering peat fire.

For peat MC of 50% (Fig. 9b), flaming ignition does not occur under the radiation of 10 $kW \cdot m^{-2}$. Instead, smoldering dominates the entire burning process, and the CO/CO_2 is always high (~0.2). Increasing the radiant heat flux to 50 $kW \cdot m^{-2}$, despite a successful flaming ignition, the flame is very weak and breaks into multiple small flamelets that do not cover the entire fuel surface. Thus, both flaming and smoldering peat fire coexist, leading to a medium level of CO/CO_2 ratio (~0.1).

4. Conclusions

In this experimental work, we found that peat soils can support a flaming wildfire, like leaves, twigs and bark, even when the peat moisture content (MC) is as high as 100%. Piloting a flame on peat is found to be more difficult than starting a smoldering peat fire, requiring a higher minimum heat flux and three times more ignition energy.

Moisture significantly lowers the flammability of peat soil. As the MC increases from 10% (air-dried) to 100% (wet), the minimum heat flux of flaming ignition increases from 7.5 $kW \cdot m^{-2}$ to 53 $kW \cdot m^{-2}$, the ignition temperature increases significantly from 285°C to 690°C; and the minimum flaming ignition energy increases from 0.3 $MJ \cdot m^{-2}$ to 2.0 $MJ \cdot m^{-2}$. The critical mass flux of flaming ignition is found to be insensitive to peat MC, but increases linearly with the heat flux, as $\dot{m}''_{ig,f} = 3.4 + 0.13\dot{q}''_r$. These phenomena suggest that defining a constant ignition temperature or mass flux is inappropriate for wet wildland fuels.

The heat of flaming combustion for dry peat is estimated to be 13 $MJ \cdot kg^{-1}$, similar to its heat of smoldering combustion (12 $MJ \cdot kg^{-1}$). The heat release rate of peat flame is significantly lower than that of pine needles, wood, and other wildland fuels, suggesting that the peat flame is weak and easy to suppress. Also, the CO/CO_2 ratio of flaming peat fires is less than 0.02, much smaller than 0.2 of smoldering peat fires. In our future work, experiments will be conducted to quantify the ignition temperature, and rate of flame spread over peat soil under external radiation. Also, future numerical simulations are needed to understanding the minimum heat flux, critical mass flux, and the interaction between flaming and smoldering peat fire.

Acknowledgment

This study received financial support from the National Natural Science Foundation of China (NSFC No.

51876183) and HK PolyU (1-BE04). The authors thank Dr. Wei Gao (Univ. of Science and Technology of China) for conducting thermal analysis for the peat sample.

Conflicts of Interest

The authors declare no conflicts of interest.

References

Babrauskas V (2001) Ignition fo Wood: A Review of the State of the Art. *Journal of Fire Protection Engineering* **12**, 81–88. doi:10.1106/104239102028711.

Babrauskas V (2016) The Cone Calorimeter. 'SFPE Handbook of Fire Protection Engineering'. (Ed M Hurley) pp. 952–980. (Springer: London) doi:10.1007/978-1-4939-2565-0.

Ballhorn U, Siegert F, Mason M, Limin S., Limin S (2009) Derivation of burn scar depths and estimation of carbon emissions with LIDAR in Indonesian peatlands. *Proceedings of the National Academy of Sciences of the United States of America* **106**, 21213–21218. doi:10.1073/pnas.0906457106.

Boonmee N, Quintiere JG (2002) Glowing and flaming autoignition of wood. *Proceedings of the Combustion Institute* **29**, 289–296. doi:10.1016/S1540-7489(02)80039-6.

Chung YJ, Spearpoint M (2008) Combustion properties of native Korean wood species. *International Journal on Engineering Performance-Based Fire Codes* **9**, 118–125.

Dimitrakopoulos AP, Papaioannou KK (2001) Flammability Assessment of Mediterranean Forest Fuels. *Fire Technology* **37**, 143–152. doi:10.1023/A:1011641601076.

Drysdale D (2011) 'An Introduction to Fire Dynamics.' (John Wiley & Sons, Ltd: Chichester, UK) doi:10.1002/9781119975465.

Fateh T, Richard F, Batiot B, Rogaume T, Luche J, Zaida J (2016) Characterization of the burning behavior and gaseous emissions of pine needles in a cone calorimeter - FTIR apparatus. *Fire Safety Journal* **82**, 91–100. doi:10.1016/j.firesaf.2016.03.008.

Fernandez-Pello AC (2017) Wildland fire spot ignition by sparks and firebrands. *Fire Safety Journal* 0–1. doi:10.1016/j.firesaf.2017.04.040.

Finney MA, Cohen JD, McAllister SS, Jolly WM (2013) On the need for a theory of fire spread. *International Journal of Wildland Fire* **2013**, 25–36. doi:10.1071/WF11117.

Frandsen WH (1987) The influence of moisture and mineral soil on the combustion limits of smouldering forest duff. *Canadian Journal of Forest Research* **16**, 1540–1544. doi:10.1139/x87-236.

Frandsen WH (1991) Heat Evolved From Smoldering Peat. *International Journal of Wildland Fire* **1**, 197–204.

Gibson CM, Chasmer LE, Thompson DK, Quinton WL, Flannigan MD, Olefeldt D (2018) Wildfire as a major driver of recent permafrost thaw in boreal peatlands. *Nature Communications* **9**, 3041. doi:10.1038/s41467-018-05457-1.

Gorham E (1994) The future of research in canadian peatlands: A brief survey with particular reference to global change. *Wetlands* **14**, 206–215. doi:10.1007/BF03160657.

Grexa O, Lübke H (2001) Flammability parameters of wood tested on a cone calorimeter. *Polymer Degradation and Stability* **74**, 427–432. doi:10.1016/S0141-3910(01)00181-1.

Hadden R, Alkatib A, Rein G, Torero JL (2012) Radiant Ignition of Polyurethane Foam: The Effect of Sample Size. *Fire Technology*. doi:10.1007/s10694-012-0257-x.

Hadden RM, Rein G, Belcher CM (2013) Study of the competing chemical reactions in the initiation and spread of smouldering combustion in peat. *Proceedings of the Combustion Institute* **34**, 2547–2553. doi:10.1016/j.proci.2012.05.060.

Holman JP (1990) 'Heat Transfer.' (McGraw-Hill: New York)

Hu Y, Christensen E, Restuccia F, Rein G (2019) Transient gas and particle emissions from smouldering combustion of peat. *Proceedings of the Combustion Institute* **37**, 4035–4042. doi:10.1016/j.proci.2018.06.008.

Hu Y, Fernandez-Anez N, Smith TEL, Rein G (2018) Review of emissions from smouldering peat fires and

their contribution to regional haze episodes. doi:10.1071/WF17084.

Huang X, Rein G (2014) Smouldering combustion of peat in wildfires: Inverse modelling of the drying and the thermal and oxidative decomposition kinetics. *Combustion and Flame* **161**, 1633–1644. doi:10.1016/j.combustflame.2013.12.013.

Huang X, Rein G (2015) Computational study of critical moisture and depth of burn in peat fires. *International Journal of Wildland Fire* **24**, 798–808. doi:dx.doi.org/10.1071/WF14178.

Huang X, Rein G (2017) Downward Spread of Smoldering Peat Fire: the Role of Moisture, Density and Oxygen Supply. *International Journal of Wildland Fire* **26**, 907–918. doi:10.1071/WF16198.

Huang X, Rein G (2019) Upward-and-downward spread of smoldering peat fire. *Proceedings of the Combustion Institute* **37**, 4025–4033. doi:10.1016/j.proci.2018.05.125.

Huang X, Rein G, Chen H (2015) Computational smoldering combustion: Predicting the roles of moisture and inert contents in peat wildfires. *Proceedings of the Combustion Institute* **35**, 2673–2681. doi:10.1016/j.proci.2014.05.048.

Huang X, Restuccia F, Gramola M, Rein G (2016) Experimental study of the formation and collapse of an overhang in the lateral spread of smouldering peat fires. *Combustion and Flame* **168**, 393–402. doi:10.1016/j.combustflame.2016.01.017.

Huggett C (1980) Estimation of rate of heat release by means of oxygen consumption measurements. *Fire and Materials* **4**, 61–65. doi:10.1002/fam.810040202.

Jacobsen RT, Lemmon EW, Penoncello SG, Shan Z, N.T. Wright (2003) Thermophysical Properties of Fluids and Materials. 'Heat Transfer Handbook'. (Eds A Bejan, AD Kraus) pp. 43–159. (John Wiley & Sons: Hoboken)

Janssens M (1991) Piloted Ignition of Wood: *Fire and Materials* **15**, 151–167. doi:10.1002/fam.810150402.

Jerry Alexander T, Martin B, Surya Theja Rao J, Ali A (2016) Development of a transformable electrically powered wheel chair into a medical emergency stretcher. *International Journal of Pharmacy and Technology* **8**, 12793–12800. doi:10.1002/fam.

Jervis FX, Rein G (2015) Experimental study on the burning behaviour of Pinus halepensis needles using small-scale fire calorimetry of live, aged and dead samples. *Fire and Materials*. doi:10.1002/fam.

Koksal K, McLennan J, Every D, Bearman C (2018) Australian wildland-urban interface householders' wildfire safety preparations: 'Everyday life' project priorities and perceptions of wildfire risk. *International Journal of Disaster Risk Reduction* 1–13. doi:10.1016/j.ijdrr.2018.09.017.

Kreye JK, Varner JM, Dugaw CJ, Engber EA, Quinn-davidson LN (2016) Patterns of Duff Ignition and Smoldering beneath Old Pinus palustris: Influence of Tree Proximity, Moisture Content, and... *Forest Science* **62**, 1–8. doi:10.5849/forsci.2016-058.

Liu Y, Stanturf J, Goodrick S (2010) Trends in global wildfire potential in a changing climate. *Forest Ecology and Management* **259**, 685–697. doi:10.1016/j.foreco.2009.09.002.

Lyon RE, Quintiere JG (2007) Criteria for piloted ignition of combustible solids. *Combustion and Flame* **151**, 551–559. doi:10.1016/j.combustflame.2007.07.020.

McAllister S (2013) Critical mass flux for flaming ignition of wet wood. *Fire Safety Journal* **61**, 200–206. doi:10.1016/j.firesaf.2013.09.002.

McAllister S, Grenfell I, Hadlow a., Jolly WM, Finney M, Cohen J (2012) Piloted ignition of live forest fuels. *Fire Safety Journal* **51**, 133–142. doi:10.1016/j.firesaf.2012.04.001.

McClure CD, Jaffe DA (2018) Investigation of high ozone events due to wildfire smoke in an urban area. *Atmospheric Environment* **194**, 146–157. doi:10.1016/j.atmosenv.2018.09.021.

Page SE, Siegert F, Rieley JO, Boehm H V., Jayak A, Limink S, Jaya A, Limin S (2002) The amount of carbon released from peat and forest fires in Indonesia during 1997. *Nature* **420**, 61–66. doi:10.1038/nature01141.1.

Pei B, Song GY, Lu C (2014) The application of cone calorimeter on the study of burning performance of liquorices. *Procedia Engineering* **71**, 291–295. doi:10.1016/j.proeng.2014.04.042.

Pel AJ, Bliemer MCJ, Hoogendoorn SP (2012) A review on travel behaviour modelling in dynamic traffic simulation models for evacuations. *Transportation* **39**, 97–123. doi:10.1007/s11116-011-9320-6.

Perdana LR, Ratnasari NG, Ramadhan ML, Palamba P, Nasruddin, Nugroho YS (2018) Hydrophilic and hydrophobic characteristics of dry peat. *IOP Conference Series: Earth and Environmental Science* **105**,. doi:10.1088/1755-1315/105/1/012083.

Prat-Guitart N, Belcher CM, Thompson DK, Burns P, Yearsley JM (2017) Fine-scale distribution of moisture in the surface of a degraded blanket bog and its effects on the potential spread of smouldering fire. *Ecohydrology* e1898. doi:10.1002/eco.1898.

Quintiere JG (2006) 'Fundamental of Fire Phenomena.' (John Wiley: New York)

Ramadhan ML, Palamba P, Imran FA, Kosasih EA, Nugroho YS (2017) Experimental study of the effect of water spray on the spread of smoldering in Indonesian peat fires. *Fire Safety Journal* **91**, 671–679. doi:10.1016/j.firesaf.2017.04.012.

Rein G (2013) Smouldering Fires and Natural Fuels. 'Fire Phenomena in the Earth System'. (Ed Claire M. Belcher) pp. 15–34. (John Wiley & Sons, Ltd.: New York) doi:10.1002/9781118529539.ch2.

Rein G (2014) Smoldering Combustion. *SFPE Handbook of Fire Protection Engineering* **2014**, 581–603. doi:10.1007/978-1-4939-2565-0_19.

Rein G, Cohen S, Simeoni A (2009) Carbon emissions from smouldering peat in shallow and strong fronts. *Proceedings of the Combustion Institute* **32**, 2489–2496. doi:10.1016/j.proci.2008.07.008.

Restuccia F, Huang X, Rein G (2017) Self-ignition of natural fuels: Can wildfires of carbon-rich soil start by self-heating? *Fire Safety Journal* **91**, 828–834. doi:10.1016/j.firesaf.2017.03.052.

Rich D, Lautenberger C, Torero JL, Quintiere JG, Fernandez-Pello C (2007) Mass flux of combustible solids at piloted ignition. *Proceedings of the Combustion Institute* **31**, 2653–2660. doi:10.1016/j.proci.2006.08.055.

Schemel CF, Simeoni A, Biteau H, Rivera JD, Torero JL (2008) A calorimetric study of wildland fuels. *Experimental Thermal and Fluid Science* **32**, 1381–1389. doi:10.1016/j.expthermflusci.2007.11.011.

Simeoni A (2016) Wildland Fires. 'SFPE Handbook of Fire Protection Engineering'. (Ed 5) pp. 3283–3302. (Springer: New York) doi:10.1007/978-1-4939-2565-0.

Tan Y, Croiset E, Douglas MA, Thambimuthu K V. (2006) Combustion characteristics of coal in a mixture of oxygen and recycled flue gas. *Fuel* **85**, 507–512. doi:10.1016/j.fuel.2005.08.010.

Thomas G (2000) Overview of Storage Development DOE Hydrogen Program: Sandia National Laboratories Livermore, California. 1–14.

Thomas JC, Hadden RM, Simeoni A (2017) Experimental investigation of the impact of oxygen flux on the burning dynamics of forest fuel beds. *Fire Safety Journal* **91**, 855–863. doi:10.1016/j.firesaf.2017.03.086.

Toledo T, Marom I, Grimberg E, Bekhor S (2018) Analysis of evacuation behavior in a wildfire event. *International Journal of Disaster Risk Reduction* **31**, 1366–1373. doi:10.1016/j.ijdrr.2018.03.033.

Turetsky MR, Benscoter B, Page S, Rein G, van der Werf GR, Watts A (2015) Global vulnerability of peatlands to fire and carbon loss. *Nature Geoscience* **8**, 11–14. doi:10.1038/ngeo2325.

Valdivieso JP, Rivera JDD (2013) Effect of Wind on Smoldering Combustion Limits of Moist Pine Needle Beds. *Fire Technology* **50**, 1589–1605. doi:10.1007/s10694-013-0357-2.

Wang S, Huang X, Chen H, Liu N (2016) Interaction between flaming and smouldering in hot-particle ignition of forest fuels and effects of moisture and wind. *International Journal of Wildland Fire* **26**, 71–81. doi:10.1071/WF16096.

Watts AC (2012) Organic soil combustion in cypress swamps: Moisture effects and landscape implications for carbon release. *Forest Ecology and Management*. doi:10.1016/j.foreco.2012.07.032.

Williams FA (1977) Mechanisms of fire spread. *Symposium (International) on Combustion* **16**, 1281–1294. doi:10.1016/S0082-0784(77)80415-3.

Wongchai P, Tachajapong W (2015) 'Effects of Moisture Content in Para Rubber Leaf Litter on Critical Mass Flux and Piloted Ignition Time.' (Elsevier B.V.) doi:10.1016/j.egypro.2015.11.517.

Zabetakis M (1965) 'Flammability characteristics of combustible gases and vapors, Bureau of Mines Bulletin 627.'

Zachar M, Martinka J, Balog K (2014) Impact of Oak wood ageing on the heat release rate and the yield of carbon monoxide during fire. **2**, 1–4.

Appendix 1. Nomenclature

Symbols		**subscripts**	
A	sample cross-section area (m^2)	a	ambient or air
E	ignition energy (MJ)	cal	theoretical calculation
h	convection coefficient ($W \cdot m^{-2} \cdot K^{-1}$)	f	flame
ΔH	heat of reaction ($MJ \cdot kg^{-1}$)	ig	ignition
$\dot{m}''$	mass flux ($g \cdot m^{-2} \cdot s^{-1}$)	$loss$	heat loss
MC	moisture content ($kg \cdot kg^{-1}$)	max	maximum
$\dot{q}''$	heat flux (kW/m^2)	min	minimum
$\dot{Q}''$	heat release rate per area ($MJ \cdot m^{-2}$)	ox	oxidation
t	time (s)	O_2	oxygen
T	temperature (°C)	py	pyrolysis
V	volumetric flow rate ($m^3 \cdot s^{-1}$)	r	radiation
X	volume fraction	sm	smoldering
ρ	density ($kg \cdot m^{-3}$)	w	water

Appendix 2. DTG and DSC analysis of peat sample

The peat sample was pulverized into powders and dried at 90°C for 48 h. The thermal analysis was conducted with a PerkinElmer STA 6000 Simultaneous Thermal Analyzer. The initial mass of peat was about 3 mg, and samples were heated at the constant rates of 30 K/min. Two oxygen concentrations were selected, 0% (nitrogen) and 21% (air), with a flow rate of 50 mL/min. Experiments were repeated twice for each case, and good repeatability is shown. Figure A1 shows the mass-loss rate (DTG) and heat flow (DSC) curves of this peat soil. Regardless of the oxygen concentration, the mass loss rate rapidly increases at around 270°C which can be defined as the pyrolysis temperature (T_{py}). The heat of smoldering (ΔH_{sm}) can be calculated by integrating the heat flow curve, and it is about 12 $MJ \cdot kg^{-1}$ for this peat.

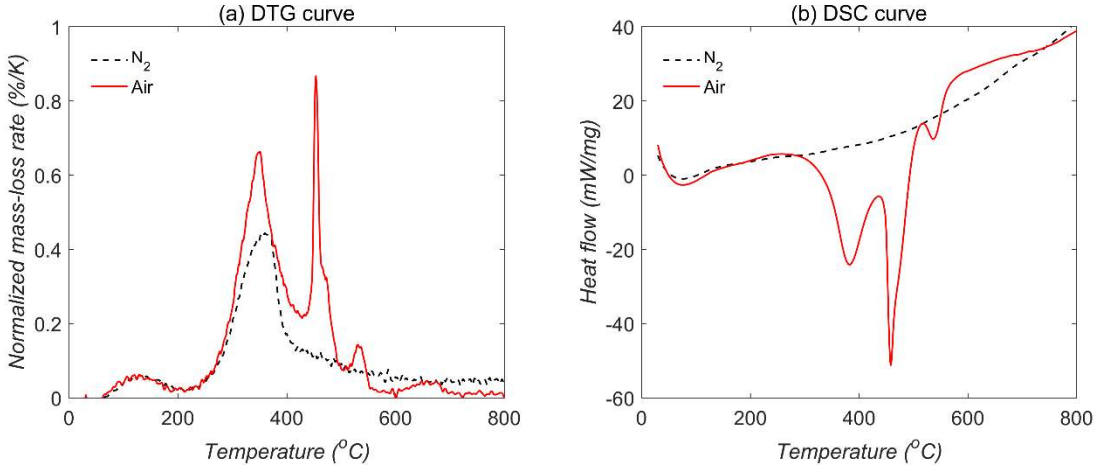

Figure A1. TGA-DSC results of peat sample under air and nitrogen ambient under the heating rate of 30 $K \cdot min^{-1}$, (a) normalized mass loss rate, and (b) heat flow as a function of temperature.